Volume 6, Issue 6, 2016, 1837 - 1841 ISSN 2069-5837

Biointerface Research in Applied Chemistry

www.BiointerfaceResearch.com

Original Research Article Open Access Journal

Received: 11.11.2016 / Revised: 06.12.2016 / Accepted: 08.12.2016 / Published on-line: 09.12.2016

Nano-nickel catalyst for the oxidation of bisphenol A to generate electricity via a fuel cell

Zheng Fan [1], Binbin Yu [1, 2], Wei Xu [1], Xingxing Wu [1], Xu Yang [1], Haoyue Zheng [1], Zucheng Wu [1, *]

[1] Department of Environmental Engineering, Laboratory of Electrochemistry and Energy Storage; State Key laboratory of Clean Energy Utilization, Zhejiang University, Hangzhou 310058, China

[2] Environmental Monitoring Center of Taizhou, Taizhou 318000, China

*corresponding author e-mail address: ***wuzc@zju.edu.cn***

ABSTRACT

The treatment of bisphenol A (BPA), a kind of harmful contaminant widely existing in soil and many solid wastes, is often energy consumption. This study is aimed to develop electrochemical declination of BPA with self-generated electricity. A nano-sized nickel catalyst was successfully synthesized to show proper activity for the oxidation, and a BPA-Cr(VI) fuel cell was assembled, in which BPA is employed as the fuel and Cr(VI) serve as the oxidant to characterize the cell property. The experimental results show that when the concentration of BPA and Cr(VI) are 4.4 mmol/L and 100 mmol/L respectively, the open circuit voltage of the fuel cell varies in the range of 1.05~1.08 V and the maximum power density of the cell is 78.1 μW/cm^2. Meanwhile, after working for about 36 h, the concentration of BPA varies from 4.4 mmol/L to 1.9 mmol/L . Under above conditions either 56% of BPA was declined or 95% of Cr(VI) was removed. This experiment demonstrates that generation of electricity and pollutant declination has been achieved successfully at the same time.

Keywords: *bisphenol A, Cr(VI), fuel cell, electricity generation, pollutant declination.*

1. INTRODUCTION

Bisphenol A (BPA) is one of the widely used industrial compounds in the world. It is mainly used for producing a variety of polymer materials such as polycarbonate, epoxy resin and unsaturated polyester resin. While polycarbonate and other materials are extensively used for manufacturing process of canned food and beverage packaging, cups, bottles, glasses and other necessities [1-4]. BPA (Scheme 1) is an endocrine disruptor that can mimic the body's own hormones and may lead to negative health effects. Therefore the US, EU, Canada, Norway and many other countries have banned the use of BPA. Furthermore, BPA migrates easily in the environment [5-7]. Due to the extensive use of BPA and it's harmful to human health, to find an appropriate treatment of BPA is still needed.

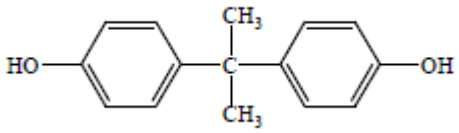

Scheme 1. The chemical structure of BPA.

According to the published literatures, at present, the main treatment methods of BPA includes absorption, biodegradation, electrolysis and photocatalytic oxidation. However, these methods either have a poor treatment effect or consume a large amount of energy [8-11]. Based on our previous research [12-13], both alkaline ethanol-Cr(VI) fuel cell and phenol-Cr(VI) fuel cell reactor can effectively achieve electricity generation and contaminant removal. The components of these "fuels" are the hydrogen atoms contained in the molecular structure of the ethanol or urea. BPA is hydrogen-rich fuel and easily be electrochemically oxidized. Therefore, attempt was made to retrieve those hydrogen atoms as electricity through an alkaline fuel cell reactor.

Phenol, BPA alike, electro-oxidation can occur at the anode relying on the electrocatalysts. Pt-noble metals or Pt-non-noble metals alloys exhibit good ability of electrocatalysts in fuel cell [14]. However, excepting for its high cost, it has been noticed that platinum demonstrates poor electrochemical performance for phenolic compounds oxidation due to the formation of a strongly adherent insulating film that passivates the surface of the electrode. Non-precious transition metals like nickel, which is much low cost, show good ability of catalysis in direct urea fuel cell [15-17]. Nickel hydroxide could catalyze oxidative removal of phenol from water [18]. In this work, nano-nickel was employed as catalyst for BPA anodic-oxidation to testify its electrocatalytic activities and to retrieve energy in BPA-Cr(VI) fuel cell. Both aqueous anode in bisphenol A solution and aqueous cathode in Cr(VI) solution were examined, through conductive wires connecting the anode and the cathode to form a circuit. It can function to retrieve electricity, reducing toxicity of contaminants. The performance of this BPA-Cr (VI) fuel cell was characterized in terms of power production performance, cogeneration of electricity and BPA and Cr (VI) removal, and the operation sustainability of this system.

This work aimed (1) to testify the abilities of nano-nickel catalyst for the electrochemical oxidation of BPA, and (2) to promote an unique BPA-Cr(VI) coupled redox fuel cell (CRFC) both to oxidize BPA and to reduce Cr(VI) and simultaneously to generate electricity.

2. EXPERIMENTAL SECTION

2.1. Experimental device. The experimental set-up is displayed in Figure 1. In this fuel cell, cathode chamber uses $K_2Cr_2O_7$ under acidic conditions as the oxidant and simply processed carbon cloth with the area of 10 cm^2 as the electrode. Anode chamber uses BPA under alkaline conditions as the fuel and Ni/C with the coating amount of 8.5 mg/cm^2 as the catalyst. A Nafion membrane is chosen as the proton exchange membrane between the cathode and anode compartments, which can effectively reduce the internal resistance of the battery.

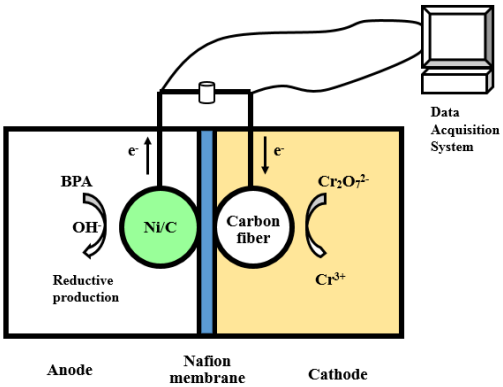

Figure 1. Schematic diagram of the BPA-Cr(VI) fuel cell device.

2.2. The preparation of electrode. The preparation of the nano Ni/C catalyst: Adding 5.0 mL $NiSO_4$ solution (0.4 mol/L), 10.0 mL sodium citrate solution (0.1 mol/L) and 250 mL deionized water into a three mouth flask and treated by 15 minutes aeration of nitrogen gas. Then dropwised 25 g 4 wt.% $NaBH_4$ solution. After stirring for 3 hours, black carbon (Carbon Vulcan XC-72R) was added into the bottle. Three hours later, the products were washed by deionized water and ethanol several times, then storing in the vacuum drying oven in 45°C for 12h.

The preparation of the electrode: adding 200 mg nickel powder, 600 μL deionized water, 1.2 mL 5% Nafion solution, 600 μL isopropanol in a centrifuge tube. Then the mixture was well stirred for 30 min in the ultrasonic mixer. The suspension was coated on the carbon cloth with 10 cm^2 effective area by brush. After dried under natural conditions for 24 h, the carbon cloth coated with the catalyst can be used as the electrode in the anode chamber. Meanwhile, the carbon cloth without catalyst can be used as the cathode electrode.

2.3. Electrochemical calculation.

(1) The cathodic efficiency (η_{cath}) was calculated as follows: [12]

$$\eta_{Cath} = \frac{Q_T}{Q_H} = \frac{[(C_0 - C_t) - (C_0 - C_{con})] \times V \times b \times F}{\frac{1}{R}\int_0^t Udt} \quad (1)$$

where Q_T is the theoretical electricity production of Cr(VI) reduction (C, Coulomb); Q_H is the total electricity production of the cell (C); C_t ,C_0 is the Cr (VI) concentration (mg/L) at time t and the initial time, respectively; C_{con} is the Cr (VI) concentration (mg/L)) at time t under control experiment; V is the volume of the catholyte (L), b is the number electrons of per mol Cr (VI) to Cr (III) (b= 3 mol e^-/mol Cr (VI)); F is the Faraday constant, 96385 C mol^{-1}.

(2) The first fitting curve of the concentration of BPA is given by:

$$c(BPA) = kx + b \quad (2)$$

where c(BPA) is the concentration of the BPA(mmol/L); x is the working time of the cell (h); k is the slope of the curve ; b is the intercept of the curve.

3. RESULTS SECTION

3.1. Characterization of nano-Ni/C catalyst for BPA oxidation.

Scanning electron microscopes (SEM) were made in order to get information on the particle size and uniformity. Fig. 2(a) show the SEM images of Ni/C catalyst. In the SEM images, numerous Ni articles were uniformly distributed on carbon though some agglomerations were observed. The X-ray diffraction (XRD) pattern of Ni/C catalyst is shown in Fig. 2. The first rather wide peak, located at the 2θ value of 25°, is attributed to the graphite (0015) facet of the Vulcan XC-72R carbon power support. The strongest diffraction peak at 2θ values of about 45° can be indexed to nickel (111) facets, which indicates the formation of nickel. There also exist another two peaks at 2θ values of about 34° and 60°, respectively, these peaks are attributed to $Ni(OH)_2$ (100) and (110) facets [19].

The average size of the Ni is calculated on the basis of the broadening of the (111) diffraction peaks according to Scherrer's equation (3):

$$d = \frac{0.9\lambda}{B_{2\theta} COS\theta_{\max}} \quad (3)$$

Where d is the average size of the particle, λ is the wavelength of X-ray, θ is the angle of Ni (111) diffraction peak, $B_{2\theta}$ is the width of the peak at half height. The average size of Ni/C particles was calculated to 4.2 nm.

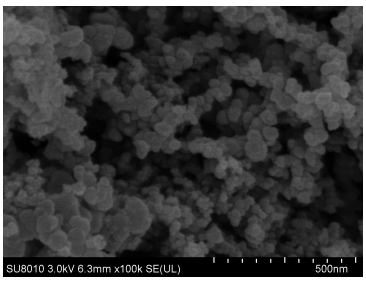

Figure 2(a). SEM images of Ni/C catalyst.

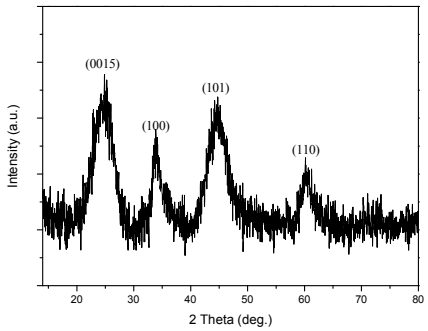

Figure 2(b). XRD pattern of nano-sized nickel supported on carbon black prepared by a chemical reduction method.

3.2. The electrochemical properties of BPA. Cyclic voltammetry (CV) has been employed to analyze and confirm the electrochemical activity of catalysts and the electrochemical activity of anode fuel. The test was carried out by using a three-electrode system, including a working electrode, a reference electrode and a counter electrode. A certain amount of the catalyst was coated on the glassy carbon electrode, then scanning in BPA solution for cyclic voltammograms. The cyclic voltammogram of Ni/C catalysts is shown in Figure 3. The main oxidation peak of BPA is at 0.615 V (vs. SCE), illustrating that Ni/C catalysts show certain catalytic properties of BPA.

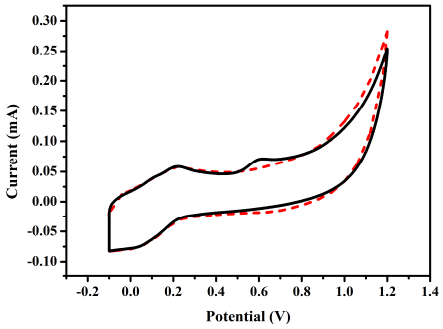

Figure 3. Cyclic voltammograms of BPA obtained at GC electrode in a solution with 0.2 mol/L PBS (loading with 2.83 mg/cm^2 Ni/C, sweep rate: 50 mV/s. Dashed line represent background current in 0.2 mol/L PBS solution, pH =7).

3.3. The electricity production performance of BPA-Cr(VI) CRFC and the removal rate of Cr(VI). In the BPA-Cr(VI) CRFC, the amount of BPA in anode chamber was excessive to test the performance of the cell. In the catholyte, the concentration of Cr(VI) and H_2SO_4 were fixed at 2.88 mmol/L and 0.5 mol/L respectively. Because the Ni/C catalyst is more stable under alkaline conditions than under acidic conditions, meanwhile the solubility of BPA in 0.2 mol/L PBS is low and in alkaline conditions the solubility is greatly increased. Therefore the system where BPA is excessive will use the alkaline medium. During the experiment, BPA's concentration in anolyte changed from 88 mmol/L to 44 mmol/L and the concentration of NaOH was controlled at 0.2 mol/L. The variation of cell voltage with time under different initial BPA concentrations is shown in Figure 4. When the concentration of BPA is 88 mmol/L and 44 mmol/L, the average open circuit voltage of the system is 0.83 V and 0.78 V respectively. After connecting 1 kΩ external resistors, the two voltages are 0.34 V and 0.21 V respectively. With the operating time of the cell extended, lower concentration of BPA corresponds to a lower voltage value and the downward trend of the voltage is more obvious. After 10 h, the voltage of the system reduces to 0.14 V and 0.12 V respectively.

When there is an electrical current obviously going through the battery, the electrode balance is broken up. The electrode potential will deviate from the equilibrium value, and the electrode reaction will be in the state of irreversible. Furthermore, as the current density increases, so does the irreversibility of the electrode reaction. The phenomenon that the electrode potential deviates from the equilibrium value caused by the current through the electrode is known as the polarization of electrode. The experiment explored the polarization curve of the cell. As what is shown in Figure 5, with the increase of the current density, the voltage of the cell is gradually decreased. It indicates that a layer of high resistance passivation film is generated on the electrode surface. Figure 5 also shows the power density of the cell. When the concentration of BPA and Cr(VI) are 44 mmol/L and 2.88 mmol/L respectively, the maximum power density of the cell is 0.4 μW/cm^2 meanwhile the current density is 1.42 μA/cm^2. While, in the 88 mmol/L BPA-2.88 mmol/L Cr (VI) system, when the current is 0.32 mA and the external resistor is 1KΩ, the power density of the cell is 1.02×10^{-2} mW/cm^2.

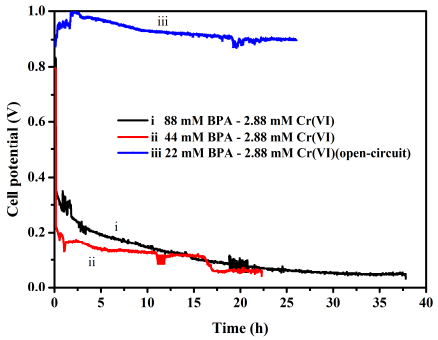

Figure 4. Variation of cell voltage with time under different initial BPA concentrations (88 mmol/L BPA (black) 44 mmol/L BPA (red) in 0.2 mol/L NaOH solution and fixing Cr (VI) at 2.88 mmol/L in 0.5 mol/L H_2SO_4).

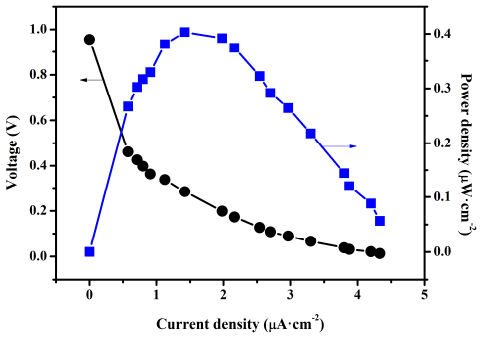

Figure 5. Polarization curve and power profiles of cell (Cathode: 2.88 mmol/L Cr(VI) + 0.5 mol/L H_2SO_4. Anode: 44 mmol/L BPA + 0.2 mol/L NaOH)

The concentration of Cr(VI) in cathode with time under the three different systems was also investigated. The change of Cr(VI)'s concentration with time was varied as shown in Figure 6. When the Cr(VI)'s concentration is fixed at 2.88 mmol/L, and set at the open circuit, the concentration of Cr(VI) remained unchanged. It indicates that the system is generally stable. While, the decreasing rates of Cr(VI)'s concentration are significantly different when the concentration of BPA in anolyte changed from 88 mmol/L to 44 mmol/L. When loaded with a 1 kΩ resistor and the concentration of BPA is 88 mmol/L, after working nearly 25 h, the removal rate of Cr(VI) is 95%. Moreover, after 40 h's work, the concentration of Cr(VI) reduced to 0.007 mmol/L and the removal rate can reach 99.7%. While, when BPA's concentration is 44 mmol/L, the removal rate of Cr(VI) slows down. After working 23 h, the removal rate is only 56%. And after 35 h, the removal rate reaches 77%.

The concentration of BPA was fixed at a certain value and changed the concentration of Cr(VI) to compare the variation of cell voltage with time under different initial Cr(VI) concentrations. As shown in Figure 6, when the concentration of Cr(VI) changed from 2.88 mmol/L to 0.96 mmol/L, the decrease of the open circuit voltage is not obvious. However, after connecting external resistors, the decrease of the voltage in the two systems is more

obvious. Basically, there are 0.04 V voltage differences. For the system in which the concentration of Cr(VI) in catholyte is 0.96 mmol/L, after 10 h continuous working, the cell voltage will reduce to below 0.1 V. Analysis of the concentration of the remaining Cr (VI) also found that, after 22 h work, the removal rate of Cr(VI) is 91% in the system where the initial concentration of Cr(VI) is 0.96 mmol/L.

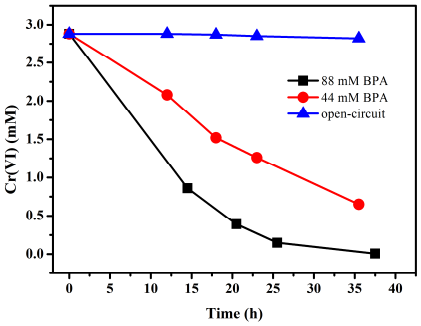

Figure 6. Cr(VI) concentration in cathode with time under different system (fixing initial Cr(VI) concentration in cathode of 2.88 mmol/L in 0.5 mol/L H_2SO_4. Anode in the system of open-circuit: 88 mmol/L BPA).

The specific electrochemical parameters during the experiment are shown in Table 1. As a result of the internal resistance of the Nafion membrane the test used is low, so the efficiency of cathode is quite high. In the system where the concentration of BPA is 88 mmol/L, the total electricity output is 12.9 C and the cathodic efficiency is 91%. Moreover, in the system where the concentration of BPA is 44 mmol/L, the total electricity output is 9.45 C and the cathodic efficiency is 74%.

3.4. The electricity production performance of BPA-Cr(VI) CRFC and the removal rate of BPA. After examining the removal rate of the Cr(VI), we changed the experiment conditions by setting the Cr(VI) in catholyte excessive to investigate the degradation of BPA. In anolyte, the concentration of BPA was fixed at 4.4 mmol/L, and the concentration of NaOH was controlled at 0.2 mol/L. Besides, in cathode, the concentration of Cr(VI) changed from 50 mmol/L to 100 mmol/L. Variation of cell voltage with time under different initial Cr(VI) concentrations is displayed in Figure 7. Setting the concentration of Cr(VI) as 50 mmol/L and 100 mmol/L respectively, the corresponding open circuit voltage of the system is 1.05 V and 1.08 V. Moreover, in the open circuit system, with time extended, the cell voltage is increasingly stable and finally reaches 1.13 V.

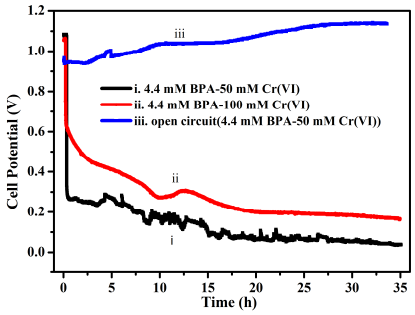

Figure 7. Variation of cell voltage with time under different initial Cr(VI) concentrations (i. 50 mmol/L Cr(VI) (black), ii. 100 mmol/L Cr(VI) (red), iii. open circuit 50 mmol/L Cr(VI) (blue) in 0.5 mol/L H_2SO_4 and fixing BPA at 4.4 mmol/L in 0.2 mol/L NaOH).

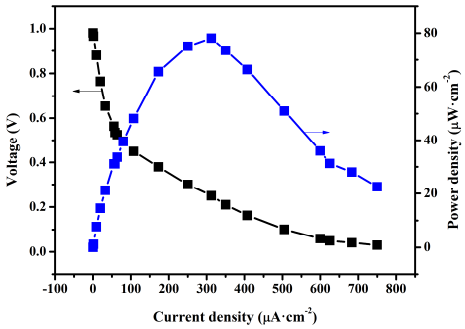

Figure 8. Polarization curve and power profiles of cell (Cathode: 100 mmol/L Cr(VI) + 0.5 mol/L H_2SO_4. Anode: 4.4 mmol/L BPA + 0.2 mol/L NaOH).

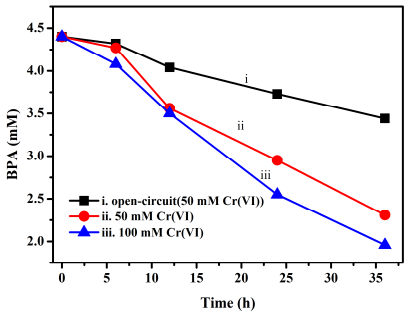

Figure 9. BPA concentration in anode with time under different system (fixing initial BPA concentration in anode of 4.4 mmol/L in 0.2 mol/L KOH).

Table 1. Cr(VI) removal efficiency and electrical parameters under different electrolytes

System[a]	C_0-Cr(VI), mmol/L	OCP, (V)	Cr(VI) removal efficiency	Total generation electricity, (C)	Electricity production of Cr(VI) reduction (C)	Cathodic efficiency, (%)
88mmol/L BPA+ Cr(VI)^{t1}	2.88	0.83	95%	12.9	11.8	91
44mmol/L BPA+ Cr(VI)^{t2}	2.88	0.78	56%	9.45	7.03	74

[a] t1=25h, t2=23h

The polarization curve and power density of the cell has been tested. As is shown in Figure 8, the maximum power density of the cell is 78.1 μW/cm^2. The change of Cr(VI)'s concentration with time under different systems is also investigated and the results are shown in Figure 9. The first order fitting curve of the concentration of BPA and correlation under different electrolytes are displayed in Table 2. Under open circuit conditions, the concentration of BPA decreased slightly. Using the first order curve to fit, the slope of the curve is -0.027. After 36 h, the concentration of remaining BPA is 78% of initial concentration. In contrast, under closed circuit condition, after working 36 h, when Cr(VI)'s concentration is 50 mmol/L and 100 mmol/L, the concentration of remaining BPA is 52% and 44% of initial concentration. The dates suggest that the fuel cell can not only generate the electricity but also achieve the goal of removing the contaminants at the same time. As for the decrease of the concentration of BPA under open circuit system, it may result from the penetration of the cell. The Nafion membrane we used in

the cell is a kind of ionic membrane, while BPA is a kind of molecule. So BPA can penetrate through the porous structure and lead to the decrease of the anolyte's concentration.

Table 2. The first order fitting curve of the concentration of BPA and correlation under different electrolytes

System	Fitting curve	Correlation coefficient (P)
50 mmol/L Cr(VI) under open circuit	y = -0.027x+4.42	0.9938
4.4 mmol/L BPA + 50 mmol/L Cr(VI)	y= -0.061x+4.44	0.9893
4.4 mmol/L BPA + 100 mmol/L Cr(VI)	y= -0.071x+4.40	0.9942

4. CONCLUSIONS

It was found that nano-sized nickel can be successfully synthesized and it is an ideal material as an anode catalyst to achieve better degradation of BPA for fuel cells.

The experimental results also show that when BPA in anode chamber is excessive, the maximum open circuit voltage of the fuel cell is varied in the range of 0.84 ~ 0.92 V. An electricity production is ca. 146.6 C/mol BPA when BPA's concentration is 88 mmol/L, after working 25 h, the removal rate of Cr(VI) with an initial concentration of 2.88 mmol/L is 95%. In contrast, when Cr (VI) in this system is excessive, the maximum open circuit voltage of the fuel cell is varied in the range of 1.05~1.08 V. When the concentration of Cr(VI) is 100 mmol/L and the BPA's concentration is 4.4 mmol/L, after working 36 h, the declination rate of BPA is 56%.

Although it has a moderate electricity generation and declination rate, the experiments demonstrate that cogeneration of electricity and pollutant removal could be simultaneously achieved via a BPA-Cr(VI) fuel cell device.

5. REFERENCES

[1] Govindaraj M., Rathinam R., Sukumar C., Uthayasankar M., Pattabhi, S., Electrochemical oxidation of bisphenol-A from aqueous solution using graphite electrodes, *Environmental Technology,* 34, 503-511, **2013**.

[2] Pereira G. F., Andrade L. S., Rocha-Filho R. C., Bocchi N., Biaggio S. R., Electrochemical determination of bisphenol A using a boron-doped diamond electrode, *Electrochimica Acta*, 82, 3-8, **2012**.

[3] Pereira G. F., Rocha-Filho R. C., Bocchi N., Biaggio S. R., Electrochemical degradation of bisphenol A using a flow reactor with a boron-doped diamond anode, *Chemical Engineering Journal*, 198, 282-288, **2012**.

[4] Yin H., Zhou Y., Xu J., Ai S., Cui L., Zhu L., Amperometric biosensor based on tyrosinase immobilized onto multiwalled carbon nanotubes-cobalt phthalocyanine-silk fibroin film and its application to determine bisphenol A, *Analytica Chimica Acta*, 659, 144-150, **2010**.

[5] Ballesteros-Gomez A., Rubio S., Perez-Bendito D., Analytical methods for the determination of bisphenol A in food, *Journal of Chromatography A,* 1216, 449-469, **2009**.

[6] Brenn-Struckhofova Z., Cichna-Markl M., Determination of bisphenol A in wine by sol-gel immunoaffinity chromatography, HPLC and fluorescence detection, *Food Additives and Contaminants*, 23, 1227-1235, **2006**.

[7] Maragou N. C., Lampi E. N., Thomaidis N. S., Koupparis M. A., Determination of bisphenol A in milk by solid phase extraction and liquid chromatography-mass spectrometry, *Journal of Chromatography A*, 1129, 165-173, **2006**.

[8] Motomitsu Kitaoka, Kiyoshi Hayashi. Adsorption of bisphenol A by cross-linked β -cyclodextrin polymer, *Journal of Inclusion Phenomena and Macrocyclic Chemistry,* 44, 429 -431, **2002**.

[9] MIke C. S., Jin M. Fujita, Biodegradation of bisphenol A in aquatic environment, *Water Science and Technology,* 42, 7-8, 31-38, **2000**.

[10] Tanaka S., Nakata Y., Kimura T., et al.. Electrochemical decomposition of bisphenol A using Pt/Ti and SnO_2/Ti anodes, *Journal of Applied Electrochemistry,* 32, 197-201, **2002**.

[11] Yoshihisa O., Isas A., Chisa N., et al.. Degradation of bisphenol A in water by TiO_2 photocatalyst. *Environmental Science and Technology,* 35, 11, 2365-2368, **2001**.

[12] Zhang H. M., Xu W., Wu Z. C., Zhou M. H., Jin T., Removal of Cr(VI) with cogeneration of electricity by an alkaline fuel cell reactor, *J. Phys. Chem. C*, 117, 14479–14484, **2013**.

[13] Yu B., Zhang H., Xu W., et al., Remediation of chromium-slag leakage with electricity cogeneration via a urea-Cr (VI) cell, *Scientific Reports,* 4, 5860, **2014**.

[14] Zhang H. M., Xu W., Fan Z., et al., Simultaneous removal of phenol and dichromate from aqueous solution through a phenol-Cr(VI) coupled redox fuel cell reactor, *Separation & Purification Technology*, 172, 152-157, **2017**.

[15] Zhang H., Xu W., Wu Z., et al. Removal of Cr(VI) with cogeneration of electricity by an alkaline fuel cell reactor, *Journal of Physical Chemistry C*, 117, 28, 14479-14484, **2013**.

[16] Yu B., Zhang H., Xu W., et al., Remediation of chromium-slag leakage with electricity cogeneration via a urea-Cr(VI) cell, *Scientific Reports,* 4, 4, 5860-5860, **2014**.

[17] Xu W., Zhang H., Li G., et al., A urine/Cr(VI) fuel cell — Electrical power from processing heavy metal and human urine, *Journal of Electroanalytical Chemistry*, 764, 38-44, **2016**.

[18] Saeed M., Ilyas M., Oxidative removal of phenol from water catalyzed by nickel hydroxide, *Applied Catalysis B Environmental,* 129, 1, 247-2254, **2012**.

[19] Xiao L., Lu J. T., Liu P. F., et al., Proton diffusion determination and dual structure model for nickel hydroxide based on potential step measurements on single spherical beads, *Journal of Physical Chemistry B*, 109, 9, 3860-7, **2005**.

6. ACKNOWLEDGEMENTS

This work is financially supported by the NSFC (Nos. 21473158, 21173188), and 863 program (No. 2013AA065900).